Cell Proliferation

Cell Prolif., 2015, **48**, 421–435 doi: 10.1111/cpr.12196

Anti-proliferative effects of γ-tocotrienol are associated with suppression of c-Myc expression in mammary tumour cells

P. Parajuli, R. V. Tiwari and P. W. Sylvester

School of Pharmacy, University of Louisiana at Monroe, Monroe, Louisiana 71209, USA

Received 20 November 2014; revision accepted 15 March 2015

Abstract

Objectives: Aberrant c-Myc activity plays a central role in cancer transformation. γ-tocotrienol is a member of the vitamin E family that displays potent anti-cancer activity. Here, studies were conducted to determine the role of c-Myc in mediating anti-proliferative effects of γ-tocotrienol in mammary cancer cells.

Materials and methods: Treatment effects on mouse +SA and human MCF-7 mammary cancer cell proliferation were determined by MTT assay and Ki-67 staining. Protein expression was determined by western blot analysis. Immunofluorescence staining and qRT-PCR were used to characterize cellular c-Myc and MYC levels respectively.

Results: Anti-proliferative effects of γ-tocotrienol were associated with reduction in total c-Myc and phosphorylated-c-Myc-serine 62, and increase in phosphorylated-c-Myc-threonine 58 levels. γ-tocotrienol also reduced PI3K/Akt/mTOR and Ras/MEK/Erk mitogenic signalling, cyclin D1 and cyclin-dependent kinase 4 levels, and increased p27 levels. However, γ-tocotrienol had no effect on MYC mRNA levels. γ-tocotrienol also increased levels of FBW7 (E3 ligase that initiates ubiquitination of c-Myc), but had no effect on serine/threonine phosphatase PP2A or isomerase Pin 1 levels. Combined treatment with GSK3α/β inhibitor LiCl or proteasome inhibitor MG132 blocked γ-tocotrienol-induced reductions in c-Myc.

Conclusions: These findings indicate that anti-proliferative effects of γ-tocotrienol are associated with reduction in c-Myc that results from increase in GSK-3α/β-dependent ubiquitination and degradation, rather than from reduction in c-Myc synthesis in +SA and MCF-7 mammary cancer cells.

Correspondence: P. W. Sylvester, School of Pharmacy, University of Louisiana at Monroe, 700 University Avenue, Monroe, Louisiana 71209, USA. Tel.: +318 342 1958; Fax: +318 342 1737; Email: sylvester@ulm.edu

Introduction

c-Myc is a multifunctional transcription factor that belongs to the basic-helix-loop-helix-zipper (bHLHZ) family of transcription factors (1). Activation of c-Myc results in its binding to a further bHLHZ protein called Myc-associated protein X or Max, to form an activated heterodimer that then translocates to the nucleus and binds to E-box sequence CACGTG to initiate gene transcription associated with a variety of cellular functions, particularly cell proliferation and survival (1,2). In normal cells, c-Myc expression and activation are highly regulated, whereas in many types of breast cancer, c-Myc is characteristically overexpressed and/or displays aberrant activity (3,4). Furthermore, RNA interference (RNAi) directed against c-Myc has been shown to significantly inhibit MCF-7 human breast cancer cell population growth in both *in vitro* and *in vivo* experimental models (5). These findings strongly suggest that targeting c-Myc may provide significant benefit as therapeutic strategy in treatment of breast cancer.

Numbers of mitogen-activated kinases are involved in stabilizing c-Myc activity, by phosphorylating it at the serine 62 amino acid residue (p-S62-c-Myc), whereas reduction in mitogen-dependent kinase activity is associated with reduction in c-Myc stability (6,7). Furthermore, mitogen-activated kinases also phosphorylate and inhibit glycogen synthetase kinase 3 (GSK3), while reduction in kinase activity results in disinhibition in GSK3 activity (8). Activated GSK3 phosphorylates c-Myc at the threonine 58 amino acid residue (p-T58-c-Myc), which results in targeting of c-Myc by E3 ubiquitin ligase, F-box/WD repeat-containing protein (FBW7) and promotes poly-ubiquitination and degradation of this transcription factor (8,9).

Previous studies have demonstrated that tocotrienols, a subgroup within the vitamin E family of compounds, induce potent anti-proliferative, apoptotic and autophagic effects on a variety of mouse and human mammary cancer cell types (10,11). Additional studies have also shown that γ-tocotrienol significantly inhibits mitogen-dependent receptor activation (ErbB2, ErbB3, ErbB4 and Met) and downstream mitogen-activated protein kinase (MAPK or Ras/MEK/Erk), phosphatidylinositol-4,5-bis-phosphate 3-kinase phosphoinositide 3-kinase (PI3K)/PI3K-dependent kinase (PDK)/protein kinase B (Akt), JAKs/Stat and NFκB mitogenic signalling (12–14).

Activation of Akt leads to phosphorylation of numerous downstream targets involved in mitogenesis, cell cycle progression and cell survival (8). One important downstream target of Akt is GSK3. GSK3 exist in several isoforms, including GSK3α and GSK3β (8). GSK3α/β is constitutively active in non-proliferating cells and phosphorylates various targets including glycogen synthase, cyclin D and c-Myc, resulting in their inactivation and metabolic degradation (8). Akt phosphorylation of GSK3α/β conversely results in inactivation of GSK3α/β, and thereby indirectly promotes activation and expression of various mitogenic transcription factors including c-Myc (8). γ-tocotrienol treatment has been shown to reduce total c-Myc protein levels in gastric and colon cancer cells (15,16). However specific effects of γ-tocotrienol on intracellular pathways involved in regulating c-Myc ubiquitination and degradation has not previously been determined in breast cancer cells. Thus, our studies were conducted to determine effects of γ-tocotrienol on c-Myc expression, stability and relationship of these effects on c-Myc in mediating anti-proliferative effects of γ-tocotrienol in mouse +SA and human MCF-7 mammary cancer cells.

Materials and methods

Reagents and antibodies

All reagents were purchased from Sigma-Aldrich (St. Louis, MO, USA), unless otherwise stated. Purified γ-tocotrienol (>98% purity) was generously provided by First Tech International Ltd. (Hong Kong, China). Although previous studies (10) have shown that δ-tocotrienol displays slightly more potent anti-cancer activity than γ-tocotrienol (IC_{50} values 3 μM versus 4 μM respectively), γ-tocotrienol was chosen for experimentation here as it is more readily available and less costly than δ-tocotrienol. Antibodies against PI3K, Akt, phospho-Akt, phospho-mTOR, phospho-Erk1/2, phospho-GSK3α/β, PP2A, phospho-Rb and p27 were purchased from Cell Signaling Technology (Beverly, MA, USA). Antibodies specific to c-Myc (9E10), MEK1/2, phospho-MEK1/2, Erk-1, Erk-2, Pin1, FBW7, Rb and Ki-67 were purchased from Santa Cruz Biotechnology, Inc. (Dallas, TX, USA). Antibodies against Max and GSKβ were purchased from GeneTex, Inc. (Irvine, CA, USA). Antibodies specific to p-S62-c-Myc and p-T58-c-Myc were purchased from Abcam (Cambridge, MA, USA); antibody to α-tubulin was purchased from Calbiochem (San Diego, CA, USA). Goat anti-rabbit and goat anti-mouse secondary antibodies were purchased from PerkinElmer Biosciences (Boston, MA, USA).

Cell lines and culture conditions

Mouse mammary +SA epithelial cell line was originally isolated from a mammary adenocarcinoma that had developed spontaneously in a BALB/c female mouse (17,18). The +SA cell line is characterized as being highly malignant, oestrogen-independent and displaying anchorage-independent growth when cultured in soft agarose gels (17,18). Culturing of these +SA and MCF-7 cells has been previously described in detail (19). Briefly, +SA cells were maintained in serum-free defined control media consisting of Dulbecco's modified Eagle's medium (DMEM/F12) supplemented with 5 mg/ml bovine serum albumin (BSA), 10 μg/ml transferrin, 100 U/ml soybean trypsin inhibitor, 100 U/ml penicillin, 0.1 mg/ml streptomycin, 10 ng/ml EGF and 10 μg/ml insulin. Oestrogen receptor-positive MCF-7 breast carcinoma cell line and MCF-10A immortalized human mammary epithelial cell line were purchased from American Type Culture Collection (ATCC, Manassas, VA, USA). MCF-7 breast cancer cells were cultured in modified Dulbecco's modified Eagle Medium (DMEM)/F12 supplemented with 10% foetal bovine serum, 100 U/ml penicillin, 0.1 mg/ml streptomycin and 10 μg/ml insulin. MCF-10A cells were maintained in DMEM/F12 supplemented with 5% horse serum, 0.5 mg/ml hydrocortisone, 20 ng/ml EGF, 100 U/ml penicillin, 0.1 mg/ml streptomycin and 10 mg/ml insulin. All cells were incubated at 37 °C in an environment of 95% air and 5% CO_2 in a humidified incubator. For subculturing, cells were rinsed twice in sterile Ca^{2+}- and Mg^{2+}-free phosphate-buffered saline (PBS) and incubated in 0.05% trypsin containing 0.025% EDTA in PBS for 5 min at 37 °C. Released cells were centrifuged, resuspended in serum-containing media, and counted using a haemocytometer.

Experimental treatment

In order to dissolve the highly lipophilic γ-tocotrienol and α-tocopherol in aqueous culture media, stock

solutions of γ-tocotrienol and α-tocopherol were prepared by suspending them in solution of sterile 10% BSA as described previously (10,19). Briefly, known amounts of γ-tocotrienol and α-tocopherol were dissolved in 100 μl absolute ethanol then added to a small volume of sterile 10% BSA in water, before being incubated at 37 °C overnight with gentle shaking. These stock solutions were used to prepare the variety of concentrations of the treatment media. Ethanol was added to all treatment groups in a given experiment so that all groups received equal volumes and final concentration of ethanol was always maintained below 0.1%. 10 mM stock solution of proteasome inhibitor MG132 was prepared in DMSO whose concentration was equalized in all treatment groups and always kept below 0.1%. 10 mM stock solution of lithium chloride (LiCl) was prepared in sterile water, and water was added to all treatment groups in a given experiment so that all groups received equal volumes.

Measurement of viable cell number

For cell population growth studies, (+SA, MCF-7 and MCF-10A) cells were initially seeded at 5×10^3 cells/well in 96-well culture plates (six wells/group) and allowed to attach overnight. The next day, cells were divided into different treatment groups and then given fresh media containing various doses of γ-tocotrienol and α-tocopherol. Cells in all groups were fed fresh treatment media every other day for a 96-h treatment period. Afterwards, viable cell number was determined using the 3-(4, 5-dimethylthiazol-2yl)-2, 5-diphenyl tetrazolium bromide (MTT) colorimetric assay, as described previously (19). Briefly, media were replaced in all treatment groups with fresh control media containing 0.5 mg/ml MTT. After 3-h incubation period, medium was removed, MTT crystals were dissolved in DMSO (100 μl/well), and optical density of each sample was measured at 570 nm, on a microplate reader (SpectraCount, Packard BioScience Company, Meriden, CT, USA) zeroed against a blank prepared from cell-free medium. Number of cells/well was calculated against a standard curve prepared by plating known cell densities, as determined by hemocytometer, in triplicate at the beginning of each experiment.

Immunocytochemical fluorescence staining

+SA and MCF-7 cells were initially plated at 1.5×10^4 cells/chamber in eight-chamber glass culture slides (BD Falcon, San Jose, CA, USA), and allowed to attach overnight. Afterwards, they were washed in PBS and incubated with control or treatment media containing 4 μM or 8 μM γ-tocotrienol for a 4-day treatment period. Fresh media were fed every other day. At the end of the treatment, all cells were washed in ice-cooled PBS, fixed in 4% paraformaldehyde/PBS for 6 min and permeabilized with 0.2% triton X-100 in PBS for 2 min. Fixed cells were washed in PBS and blocked with 5% goat or donkey serum in PBS for 1 h at room temperature. Cells were then incubated with specific primary antibodies against Ki-67 (1:800) or c-Myc (1:500) in 5% goat or donkey serum in PBS at 4 °C overnight. The next day, cells were washed five times in ice-cold PBS followed by incubation with Alexa fluor 488 (+SA)- or Alexa fluor 594 (MCF-7)-conjugated secondary antibody (1:5000) in 5% goat or donkey serum in PBS for 1 h at room temperature. All cells were then washed three times in ice-cold PBS and later mounted with Vectashield medium containing DAPI (Vector Laboratories IN., Burlingame, CA, USA). Fluorescenct images were captured using an LSM Pascal confocal microscope (Carl Zeiss Microimaging Inc., Thornwood, NY, USA). Percentages of Ki-67-labelled cells in each treatment group were determined by counting number of positive Ki-67 stained cells as proportion of total number of cells, as seen by blue DAPI staining. Cells were counted manually in five photomicrographs taken randomly in each chamber for every treatment group.

Western blot analysis

+SA, MCF-7 and MCF-10A cells were plated at 1×10^6 cells/100 mm culture dish in control media and allowed to attach overnight. The following day, they were washed in PBS and exposed to control or treatment media containing 2–20 μM γ-tocotrienol for a 4-day culture period. For analysis of cell cycle-related proteins, +SA and MCF-7 cells were initially plated at 1×10^6 cells/100 mm culture dish in control media and allowed to attach overnight. The following day, they were divided into control and treatment groups, media were removed, cells were washed and then fed fresh mitogen-free media containing 2–8 μM γ-tocotrienol to establish cell cycle synchronization in all groups (20,21). After 48-h incubation period, media were removed, cells fed their respective control or treatment media supplemented with 100 ng/ml EGF, and then collected after 24-h exposure to mitogen stimulation, as described previously (20). Then, cells were isolated with trypsin, washed in PBS, and whole cell lysates were prepared in Laemmli buffer, as described previously (22). Protein concentration in each sample was determined using a Bio-Rad protein assay kit (Bio Rad, Hercules, CA, USA). Equal amounts of protein (50 μg/lane) from each sample were then subjected to electrophoresis with

7.5–20% SDS polyacrylamide minigels. Proteins from minigels were transblotted at 30 V for 12–16 h at 4 °C on to single 8″ × 6.5″ polyvinylidene fluoride (PVDF) membranes (PerkinElmer Life Sciences, Wellesley, MA, USA) in a Trans-Blot Cell (Bio-Rad) according to the methods of Towbin *et al.* (23). These PVDF membranes were then blocked with 2% BSA in 10 mM Tris–HCl containing 50 mM NaCl and 0.1% Tween 20, pH 7.4 (TBST), then incubated with specific primary antibodies against c-Myc (9E01), p-S62-c-Myc, Max, GSK3β, phospho-GSK3α/β, phospho-T58-c-Myc, Pin1, PP2A, FBW7, PI3K, Akt, phospho-Akt, phospho-mTOR, Ras, MEK1/2, phospho-MEK1/2, Erk1, Erk2, phospho-Erk1/2, Rb, phospho-Rb, E2F1, cyclinD1, CDK4 and p27 diluted 1:1000 to 1:5000 in 2% BSA in TBST overnight at 4 °C. Membranes were incubated in primary antibodies against α-tubulin, diluted 1:5000 in 2% BSA in TBST for 2 h at room temperature. They were then washed five times in TBST and incubated with respective horseradish peroxide-conjugated secondary antibody diluted 1:5000 in 2% BSA in TBST for 1 h at room temperature followed by washing five times in TBST. Blots were then visualized by chemiluminescence according to the manufacturer's instructions (Pierce, Rockford, IL, USA). Images of protein bands from all treatment groups within a given experiment were acquired using the Syngene Imaging System (Frederick, MD, USA). Visualization of α-tubulin was used to ensure equal sample loading in each lane. Images of protein bands were acquired and scanning densitometric analysis was performed with Kodak molecular imaging software version 4.5 (Carestream Health Inc., New Haven, CT, USA). All experiments were repeated at least three times and a representative western blot image from each experiment is shown in the Figures.

Quantitative real-time PCR

For qRT-PCR studies, cells were plated at 1×10^5 cells in six-well culture plates and allowed to attach overnight. The next day, they were divided into different treatment groups (three wells/group) culture media were removed, specimens were washed in sterile PBS, cells were treated with 2–8 μM γ-tocotrienol and fresh media were fed every other day during the 4-day culture period. Total RNA was extracted using SV total RNA isolation system from Promega Corporation (Madison, WI, USA) according to the manufacturer's instructions. First-strand cDNA was generated from total RNA for each sample using the Sensiscript RT kit from Qiagen Inc. (Valencia, CA, USA) according to the manufacturer's instructions. qPCR primer pairs for human MYC (#HP206146), human GAPDH (#HP205798) mouse MYC (#MP20849) and mouse GAPDH (#MP205604) were purchased from OriGene Technologies (Rockville, MD, USA). cDNA was then amplified in triplicate for each sample with a reaction using iQ SYBR Green Supermix reagent from Bio-Rad Laboratories (Hercules, CA). qRT-PCR was performed on a iCycler iQ multicolor Real-Time PCR system from Bio-Rad Laboratories. PCR reactions consisted of an initial denaturation step (3 min at 95 °C) and 40 cycles of PCR (95 °C for 10 s, and 59.5 °C for 45 s). During thermal cycling, the threshold cycle (Ct) is defined as the cycle number when amplification of a specific PCR product is detected. Average Ct value of GAPDH was subtracted from average Ct value of target genes (MYC) to normalize the amount of sample RNA added to the reaction. Degree of change in mRNA levels in treatment *versus* control samples was calculated using the formula:

$$\text{Fold change} = 2(\Delta\text{Ct control} - \Delta\text{Ct treated})$$

Statistical analysis

Differences between groups were analysed by one-way analysis of variance (ANOVA) followed by Dunnett's *t*-test. Difference of $P < 0.05$ was considered statistically significant compared to the vehicle-treated control group, or as defined in the Figure legends.

Results

Effects of various doses of γ-tocotrienol and α-tocopherol on +SA and MCF-7 mammary tumour cell- and MCF-10A immortalized normal human mammary epithelial cell-population growth

Treatment with 3–4 μM γ-tocotrienol significantly inhibited mouse +SA mammary tumour cell population growth in dose-dependent manner compared to cells in the vehicle-treated control group (Fig. 1a). Treatment with 6–8 μM of γ-tocotrienol significantly inhibited human MCF-7 human breast cancer cell population growth in a dose-dependent manner compared to cells in the vehicle-treated control group (Fig. 1a). IC_{50} values were 3.3 μM and 7.8 μM for γ-tocotrienol-treated +SA and MCF-7 mammary cancer cells respectively. However, treatment with 5–20 μM γ-tocotrienol treatment had no significant effect the expansion of immortalized normal MCF-10A human mammary epithelia cells. Similarly, treatment with 20–100 μM α-tocopherol had no significant effect on +SA, MCF-7 or MCF-10A cell growth as compared to vehicle-treated controls in their respective groups (Fig. 1b).

Effects of γ-tocotrienol on Ki-67 immunofluorescent staining in mammary tumour cells

Ki-67 a nuclear protein, is a marker for active cell proliferation (24) and is visualized in Fig. 2a as bright red nuclear staining. Following 4-day treatment period, 4 μM (+SA) and 8 μM (MCF-7) γ-tocotrienol treatment reduced positive Ki-67 staining in both +SA and MCF7 cells, compared to cells in their respective vehicle-treated control groups (Fig. 2a). Quantitative analysis of treatment effects show that more than 80% of the cells

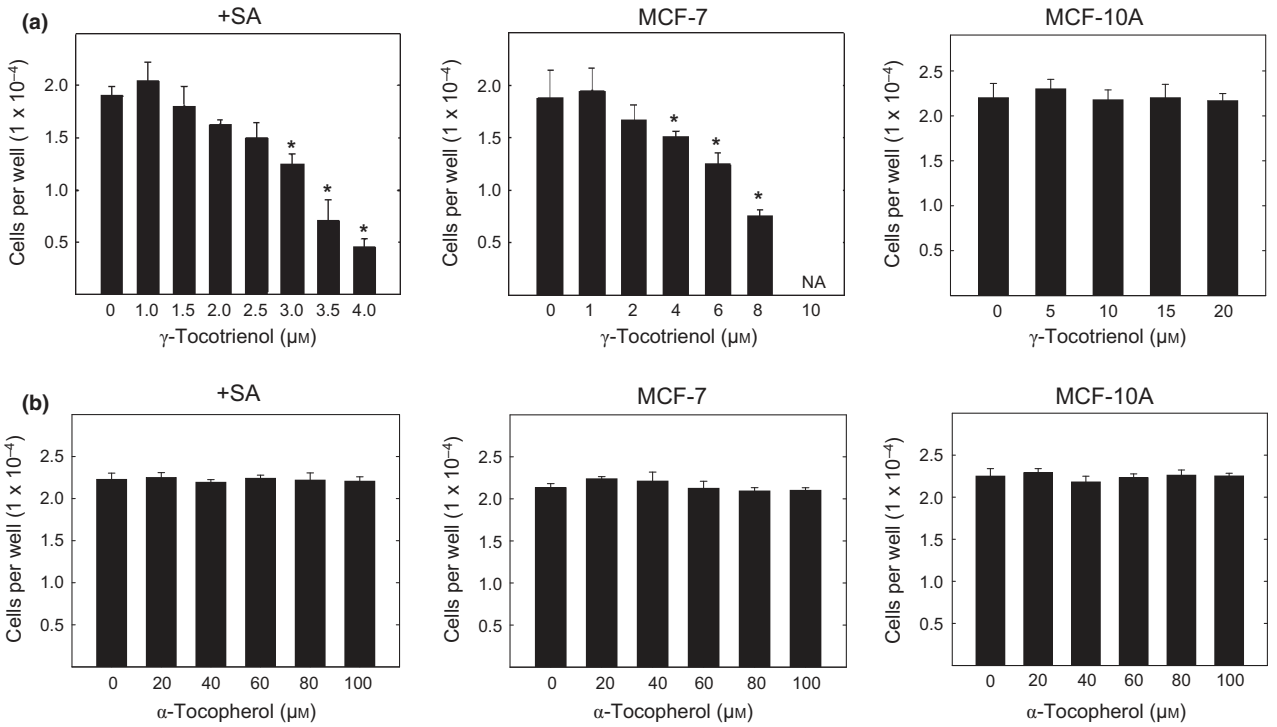

Figure 1. Anti-proliferative effects of γ-tocotrienol and α-tocopherol on +SA and MCF-7 mammary tumour and normal MCF-10A mammary epithelial cells. Vertical bars indicate mean viable cell number ± SEM in each treatment group. *$P < 0.05$ compared to their respective vehicle-treated control group.

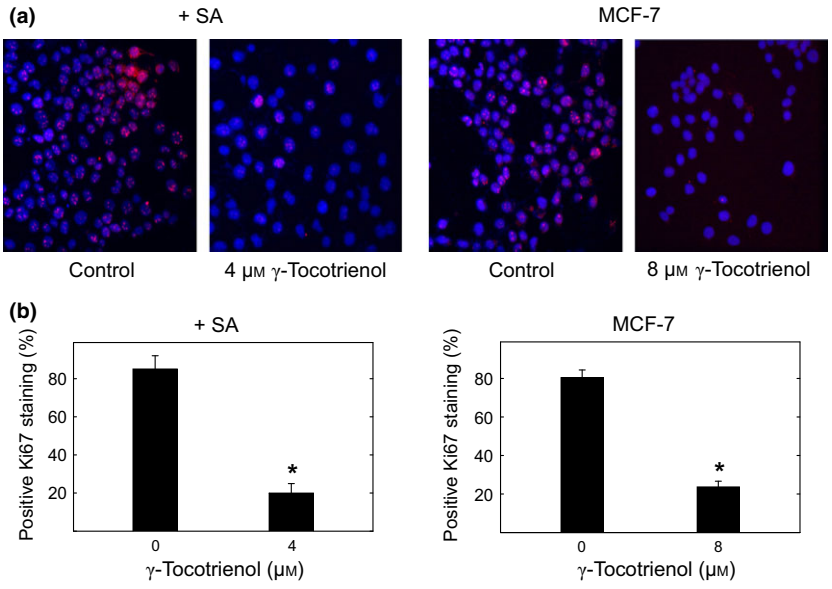

Figure 2. Effects γ-tocotrienol on Ki-67 immunofluorescence staining in +SA and MCF-7 mammary tumour cells. (a) Bright red staining visualized in the photomicrographs indicates positive staining for Ki-67, while blue represents counterstaining of cell nuclei with DAPI. Magnification of each image is 200x. (b) Percentage of +SA cells displaying positive Ki-67 staining in proportion to total number of cells within each treatment group. Cells were counted manually in five photomicrographs selected randomly in each chamber for each treatment group. Vertical bars represent percentage positive Ki-67 staining ± SEM in each treatment group. *$P < 0.05$ compared to their respective vehicle-treated control group.

had positive Ki-67 staining in +SA and MCF-7 vehicle-treated control groups (Fig. 2b). In contrast, treatment with 4 μM (+SA) and 8 μM (MCF-7) γ-tocotrienol significantly reduced positive Ki-67 to <20% of that observed in their respective vehicle-treatment control groups (Fig. 2b).

Dose–response effects of γ-tocotrienol on c-Myc, p-S62-c-Myc and Max levels in mammary tumour cells following 96-h treatment period

Western blot analysis showed that treatment with 0–4 μM (+SA) and 0–8 μM (MCF-7) γ-tocotrienol caused dose-dependent reduction in total c-Myc and p-S62 c-Myc levels, but had no effect on Max levels after 4-day exposure period (Fig. 3a). Scanning densitometric analysis of protein bands in each blot showed that treatment with 4 μM (+SA) and 8 μM (MCF-7) γ-tocotrienol induced significant reduction in total c-Myc and p-S62-c-Myc levels compared to cells in their respective vehicle-treated control groups (Fig. 3b).

Time–response effects of γ-tocotrienol on c-Myc, p-S62-c-Myc and Max levels in normal MCF-10A mammary epithelial cells, and +SA and MCF-7 mammary tumour cells

Western blot analysis also showed that treatment with 4 μM (+SA) and 8 μM (MCF-7) γ-tocotrienol caused time-dependent reduction in total c-Myc and p-S62 c-Myc levels, but had no effect on Max levels (Fig. 4a). In contrast, treatment with 20 μM γ-tocotrienol had no effect on c-Myc, p-S62 c-Myc levels and Max levels in MCF-10A cells at any time during the 96-h treatment period (Fig. 4a). Scanning densitometric analysis of protein bands in each blot showed that treatment with 4 μM (+SA) and 8 μM (MCF-7) γ-tocotrienol induced significant reduction in total c-Myc and p-S62-c-Myc levels by 72 and 96 h after treatment exposure compared to cells in their respective vehicle-treated control groups (Fig. 4b). No significant treatment effects were observed in MCF-10A cells (Fig. 4b).

Effects of γ-tocotrienol on c-Myc immunofluorescence staining in mammary tumour cells

Positive nuclear c-Myc immunofluorescent staining was observed in both +SA (bright red) and MCF-7 (bright green) mammary tumour cells maintained in control culture media (Fig. 5). However, treatment with 4 μM (+SA) or 8 μM (MCF-7) γ-tocotrienol induced nearly complete inhibition in positive c-Myc staining in these cells compared to their respective vehicle-treated control groups (Fig. 5).

Effects of γ-tocotrienol on MYC mRNA levels in mammary tumour cells

Treatment effects on MYC mRNA levels in mouse +SA and human MCF-7 mammary tumour cells, as determined by qRT-PCR analysis, are shown in Fig. 5. Following 4-day exposure to 0–4 μM (+SA) or 0–8 μM

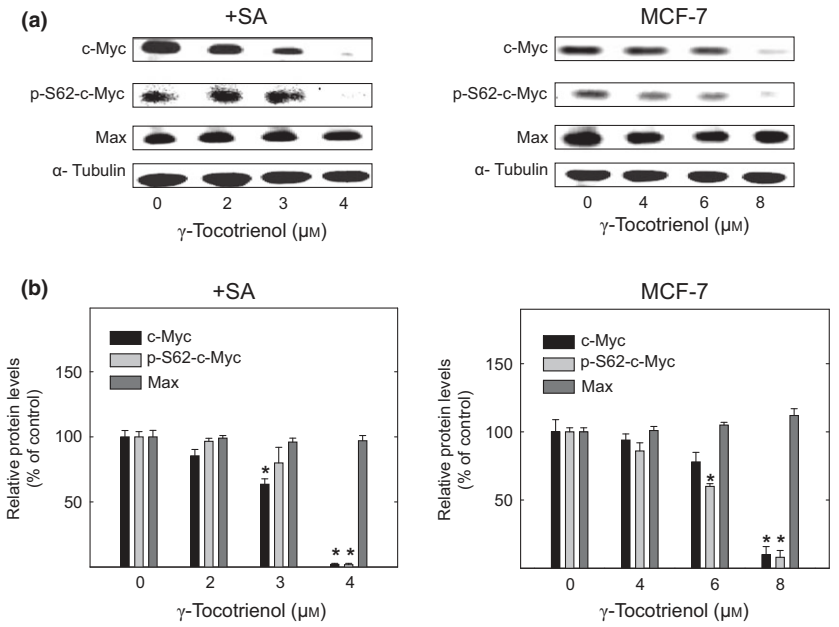

Figure 3. (a) Western blot analysis of γ-tocotrienol dose–response effects on relative levels of c-Myc, p-S62 c-Myc and Max in +SA and MCF-7 mammary tumour cells after 96-h treatment period. Following experimental treatment, whole cell lysates were prepared for subsequent separation by polyacrylamide gel electrophoresis (50 μg/lane) followed by western blot analysis. (b) Scanning densitometric analysis was performed on all blots performed in triplicate, and integrated optical density of each band was normalized with corresponding α-tubulin, as shown in bar graphs below their respective western blot images. Vertical bars indicate normalized integrated optical density of bands visualized in each lane ± SEM. $*P < 0.05$ compared to their respective vehicle-treated control groups.

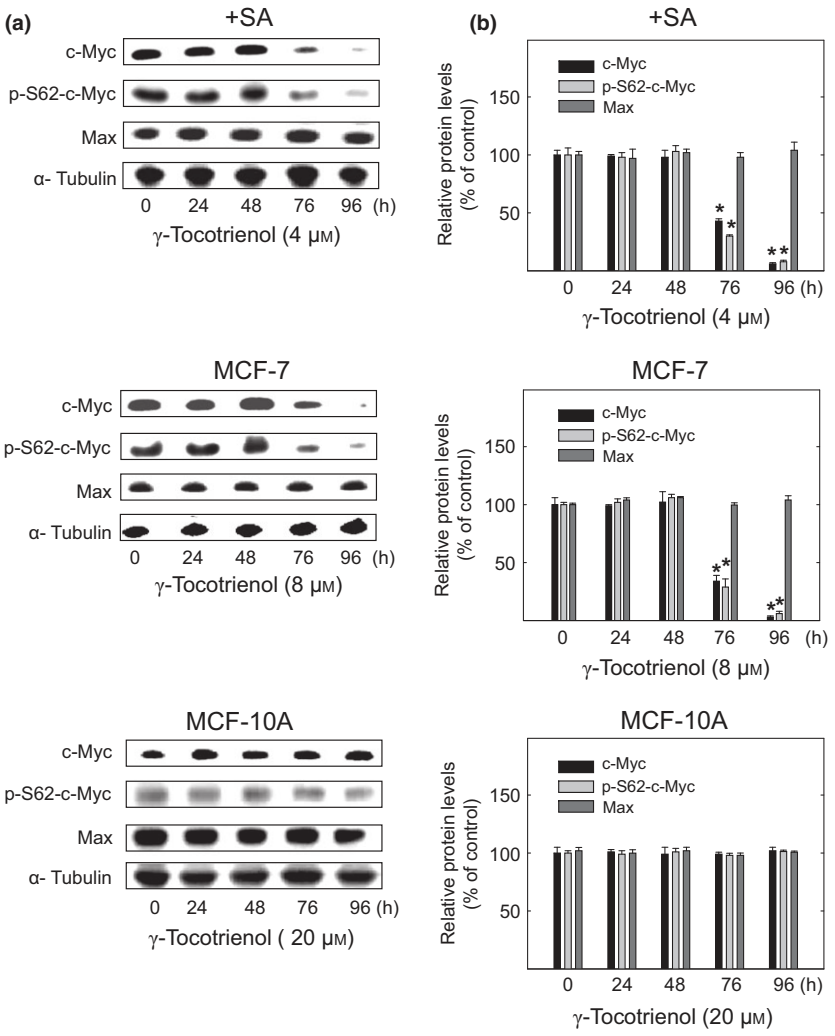

Figure 4. (a) Western blot analysis of γ-tocotrienol time–response effects on relative levels of c-Myc, p-S62 c-Myc and Max in +SA and MCF-7 mammary tumour and normal MCF-10A mammary epithelial cells. Whole cell lysates were collected at specified time points and were subjected to subsequent separation by polyacrylamide gel electrophoresis (50 μg/lane) followed by western blot analysis. (b) Scanning densitometric analysis was performed on all blots performed in triplicate and the integrated optical density of each band was normalized with corresponding α-tubulin, as shown in bar graphs below their respective western blot images. Vertical bars indicate normalized integrated optical density of bands visualized in each lane ± SEM. $*P < 0.05$ compared to their respective vehicle-treated control groups.

(MCF-7) γ-tocotrienol, MYC mRNA levels showed no significant differences between treatment groups within their respective mammary tumour cell lines (Fig. 6).

Effects of γ-tocotrienol on intracellular levels of GSK3β, phospho-GSK3α/β, p-T58-c-Myc, Pin 1 PP2A and FBW7 in mammary tumour cells

Effects of 4-day exposure to growth inhibitory doses of γ-tocotrienol on intracellular levels of key proteins involved in modulating c-Myc protein stability and degradation, in +SA and MCF-7 mammary tumour cells, are shown in Fig. 7. Western blot analysis showed that treatment with 0–4 μM (+SA) and 0–8 μM (MCF-7) γ-tocotrienol had no effect on intracellular levels of total GSK3β, Pin 1 or PP2A (Fig. 7a). However, these same treatments induced dose-responsive increase in p-T58-c-Myc (unstable/inactive) and FBW7, and corresponding reduction in phospho-GSK3α/β (inactive) levels, compared to cells in their respective vehicle-treated control groups (Fig. 7a). Scanning densitometric analysis of protein bands in each blot showed that treatment with 3–4 μM (+SA) and 6–8 μM (MCF-7) γ-tocotrienol induced significant increase in p-T58-c-Myc and FBW7, and corresponding significant reduction in phospho-GSK3α/β levels compared to cells in their respective vehicle-treated control groups (Fig. 7b).

Effects of γ-tocotrienol, MG132 and LiCl alone or in combination on c-Myc levels in mammary tumour cells

Treatment with 3 μM MG132 (a proteasome inhibitor), alone, had no significant effect, whereas treatment with 4 μM (+SA) and 8 μM (MCF-7) γ-tocotrienol alone significantly reduced c-Myc expression after 4-day culture period (Fig. 8a). However, pre-treatment with 3 μM MG132 for 6 h prior to γ-tocotrienol exposure caused nearly complete blockade of inhibitory effects of

γ-tocotrienol on c-Myc protein expression in both +SA and MCF-7 mammary tumour cell lines (Fig. 8a). Treatment with 2 mM LiCl, a GSK3β inhibitor, alone had little or no effect, whereas treatment with 4 μM (+SA) and 8 μM (MCF-7) γ-tocotrienol alone significantly reduced c-Myc expression after 4-day culture period (Fig. 8b). Combined treatment with these same doses of LiCl and γ-tocotrienol caused complete blockade of inhibitory effects of γ-tocotrienol on c-Myc protein expression in both +SA and MCF-7 mammary tumour cell lines (Fig. 8b).

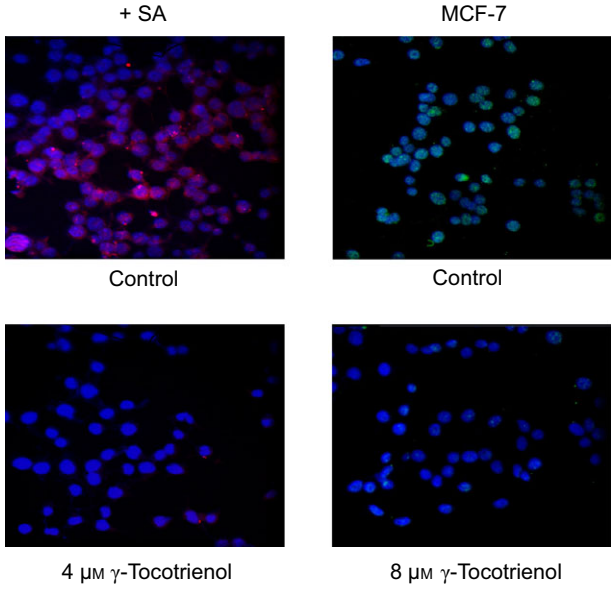

Figure 5. Effects of γ-tocotrienol on c-Myc immunofluorescent staining in +SA and MCF-7 mammary tumour cells. Following treatment exposure, cells were fixed, blocked and incubated with specific primary antibody for c-Myc followed by incubation with Alexa Flour 594 (+SA)- or 488 (MCF-7)-conjugated secondary antibodies. Bright red (+SA) or green staining (MCF-7) visualized in the photomicrographs indicates positive staining for c-Myc, while blue represents counterstaining of cell nuclei with DAPI. Magnification of each image is 200x.

Effects of γ-tocotrienol on PI3K/Akt/mTOR mitogenic signalling in mammary tumour cells

Western blot analyses shows that treatment with 0–4 μM (+SA) or 0–8 μM (MCF-7) γ-tocotrienol had little or no effect on total Akt levels, but caused a relatively large dose-responsive reduction in PI3K, phospho-Akt (active) and phospho-mTOR (active) levels in these mammary tumour cell lines (Fig. 9a). Scanning densitometric analysis of protein bands in each blot showed that treatment with 3–4 μM (+SA) and 6–8 μM (MCF-7) γ-tocotrienol induced significant reduction in PI3K, phospho-Akt and phospho-mTOR levels compared to cells in their respective vehicle-treated control groups (Fig. 9b).

Effects of γ-tocotrienol on Ras/MEK/Erk mitogenic signalling in mammary tumour cells

Western blot analyses shows that treatment with 0–4 μM (+SA) or 0–8 μM (MCF-7) γ-tocotrienol was found to have little or no effect on total Ras, MEK1/2, Erk1 and Erk2 levels, but caused a relatively large dose-responsive reduction in phospho-MEK1/2 (active) and phospho-Erk1/2 (active) levels in +SA and MCF-7 mammary tumour cells (Fig. 10a). Scanning densitometric analysis of protein bands in each blot showed that treatment with

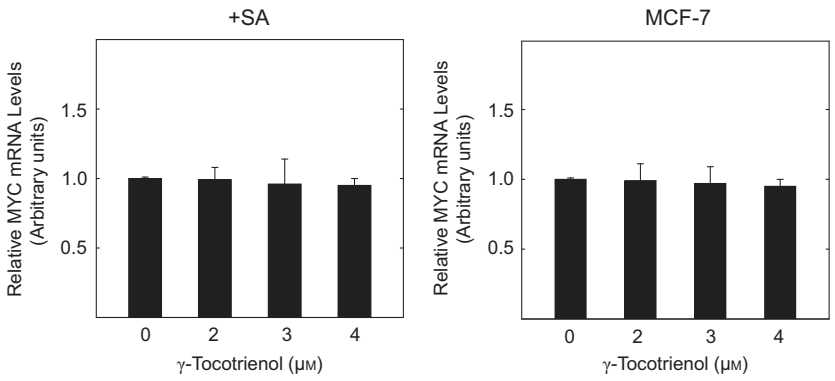

Figure 6. qRT-PCR analysis of γ-tocotrienol effects on relative levels of MYC mRNA in +SA and MCF-7 mammary tumour cells. Following treatment exposure, total RNA was extracted from cells and first-strand cDNA was generated from total RNA for each sample according to the instructions provided by the manufacturer. MYC and GAPDH mRNA were measured using iCycler iQ multicolor Real-Time PCR system. Changes in mRNA levels of MYC were normalized to mRNA level of GAPDH, and relative fold change in mRNA level was calculated compared to their respective vehicle-treated controls. Vertical bars indicate relative fold change in mRNA ± SEM (arbitrary units) in each treatment group for each given cell line.

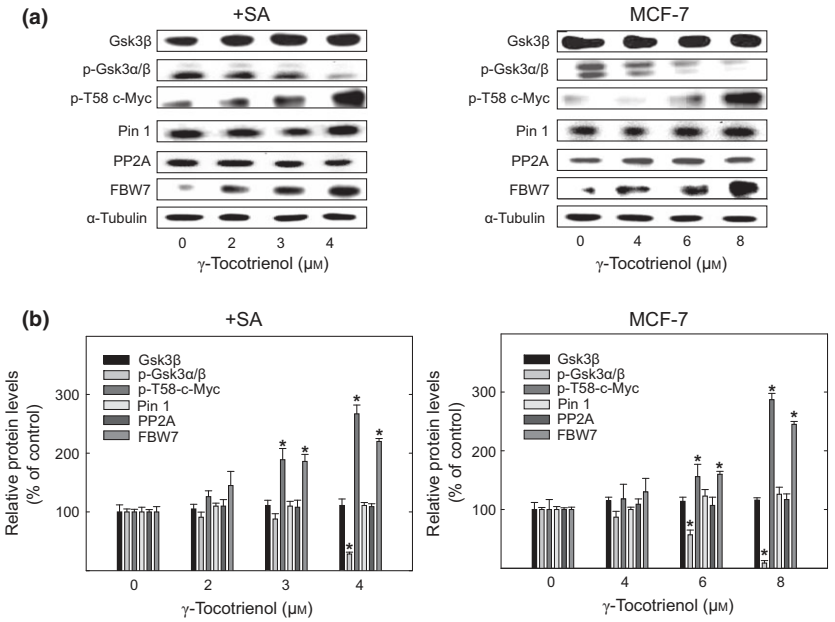

Figure 7. Western blot analysis of γ-tocotrienol effects on expression of proteins involved in c-Myc degradation pathway in +SA and MCF-7 mammary tumour cells. After treatment exposure, whole cell lysates were prepared for subsequent separation by polyacrylamide gel electrophoresis (50 μg/lane) followed by western blot analysis for GSK3β, phospho-GSK3α/β (p-GSK3α/β), p-T58 c-Myc, Pin 1, PP2A and FBW7. Scanning densitometric analysis was performed in triplicate on all blots and integrated optical density of each band was normalized with corresponding α-tubulin levels, as shown in bar graphs below their respective western blot images. Vertical bars indicate the normalized integrated optical density of bands visualized in each lane ± SEM. $*P < 0.05$ compared to their respective vehicle-treated control groups.

3–4 μM (+SA) and 6–8 μM (MCF-7) γ-tocotrienol induced significant reduction in phospho-MEK1/2 and phospho-Erk1/2 levels compared to cells in their respective vehicle-treated control groups (Fig. 10b).

Effects of γ-tocotrienol on Rb, phospho-Rb, E2F1, CDK4, cyclin D1 and p27 in mammary tumour cells

Effects of 4-day exposure to growth inhibitory doses of γ-tocotrienol on intracellular levels of key proteins involved cell cycle progression in +SA and MCF-7 mammary tumour cells are shown in Fig. 11. Western blot analyses indicate that treatment with 0–4 μM (+SA) or 0–8 μM (MCF-7) γ-tocotrienol induced dose-responsive reductions in levels phospho-Rb (inactive), E2F1, CDK4, and cyclin D1, and corresponding increase in p27 levels (Fig. 11a). However, these same treatments caused little or no change in total Ras and Rb levels in + SA and MCF-7 mammary tumour cells (Fig. 11a). Scanning densitometric analysis of protein bands in each blot showed that treatment with 3–4 μM (+SA) and 6–8 μM (MCF-7) γ-tocotrienol induced significant reduction in phospho-Rb (active), E2F1, CDK4 and cyclin D1, and corresponding significant increase in p27 levels compared to cells in their respective vehicle-treated control groups (Fig. 11b).

Discussion

Results of the present investigation demonstrate that the anti-proliferative effects of γ-tocotrienol were directly associated with reduction in c-Myc levels in mouse +SA and human MCF-7 mammary tumour cells. This reduction in c-Myc levels appeared to result from γ-tocotrienol-dependent increase in c-Myc degradation, rather than from reduction in c-Myc synthesis. Experimental findings obtained from qRT-PCR studies showed that γ-tocotrienol treatment had no effect on MYC mRNA, an indication that c-Myc synthesis was not affected. Furthermore, γ-tocotrienol exposure resulted in reduction PI3K/Akt/mTOR and Ras/MEK/Erk mitogenic signalling and corresponding lowering of p-S62-c-Myc, an oncogenic and stable form of c-Myc. γ-tocotrienol treatment was also shown to cause reduction in phosphorylated GSK3α/β (inactive) levels (indication of disinhibition in GSK3α/β activity), and corresponding increase in p-T58-c-Myc (inactive and unstable form of c-Myc) targeted for degradation. Exposure to γ-tocotrienol also caused increase in FBW7 levels (E3 ligase that initiates ubiquitination and subsequent degradation of c-Myc). In addition, treatment doses of γ-tocotrienol used in the present study are physiologically relevant based on serum concentrations of tocotrienols that have been found to range between 2 and 4 μM in individuals given a single oral dose of mixed tocotrienols (300 mg) under fed or fasted conditions (25). These findings demonstrate that anti-proliferative effects of γ-tocotrienol were associated with reduction in c-Myc resulting from increase in GSK-3α/β-dependent ubiquitination and degradation. This suggestion is further enhanced by the finding that combined treatment with proteasome inhibitor MG132

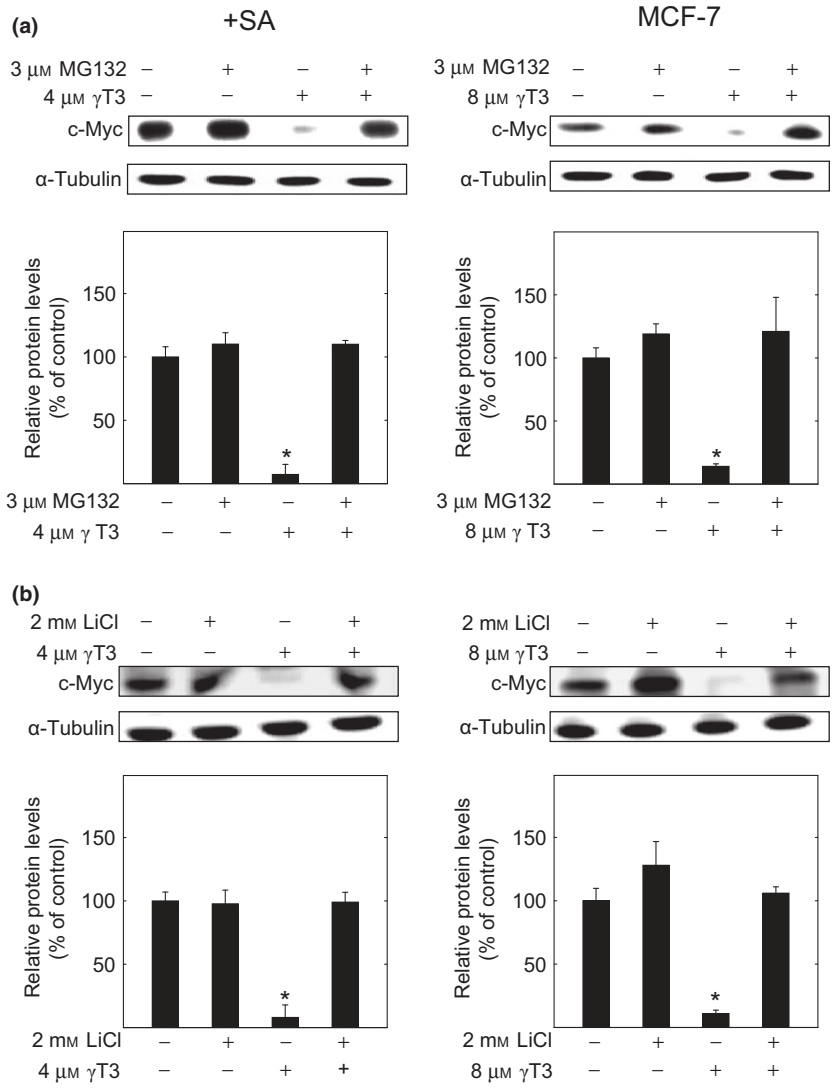

Figure 8. Western blot analysis of γ-tocotrienol (γT3), MG123 (a proteasome inhibitor) and LiCl (a GSK3β inhibitor) effects on c-Myc expression in +SA and MCF-7 mammary tumour cells. (a) +SA and MCF-7 cells were divided into different groups and treated with 0–3 μM MG132 for 6 h prior to exposure to 0–4 μM (+SA) or 0–8 μM (MCF-7) γ-tocotrienol for 4-day exposure period. (b) +SA and MCF-7 cells were divided into different groups and treated with 0–2 mM LiCl in combination with 0–4 μM (+SA) or 0–8 μM (MCF-7) γ-tocotrienol for a 4-day exposure period. Afterwards, whole cell lysates were prepared for subsequent separation by polyacrylamide gel electrophoresis (50 μg/lane) followed by western blot analysis for c-Myc. Scanning densitometric analysis was performed in triplicate on all blots and the integrated optical density of each band was normalized with corresponding α-tubulin levels, as shown in bar graphs below their respective western blot images. Vertical bars in the graph indicate the normalized integrated optical density of bands visualized in each lane ± SEM. $*P < 0.05$ compared to their respective vehicle-treated control groups.

or GSK3α/β inhibitor LiCl blocked inhibitory effects of γ-tocotrienol on c-Myc expression.

Previous studies in MYC transgenic mice have shown that overexpression of c-Myc promoted development of invasive mammary adenocarcinomas, whereas inhibition of c-Myc expression resulted in spontaneous regression of existing mammary tumours in these mice (3). In addition, primary breast cancers characteristically display elevation in p-S62-c-Myc and corresponding reduction in p-T58-c-Myc levels (9). Specifically, p-S62-c-Myc levels have been found to be elevated in 21 of 26 human breast cancer cell lines examined, and treatment with siRNA directed against MYC resulted in significant dose-dependent inhibition in growth of breast cancer cell lines overexpressing p-S62-c-Myc (26). Results from the present study indicate that γ-tocotrienol-induced suppression of total c-Myc and p-S62-c-Myc levels directly correlated to reduction in +SA and MCF-7 mammary tumour cell popualtion growth and positive Ki-67 staining, a marker for active mitogenesis (24). However, γ-tocotrienol treatment had no effect on intracellular level of ubiquitous c-Myc binding partner Max, suggesting that γ-tocotrienol acted selectively to reduce total c-Myc and p-S62-c-Myc levels in these cancer cells.

GSK-3 plays a key role in c-Myc degradation (6,9). Activated GSK3 phosphorylates c-Myc at amino acid residue T58, which then promotes c-Myc binding to E3 ubiquitin ligase, FBW7, which leads to poly-ubiquitination and proteasomal degradation of this transcription factor (8,9,27,28). Some studies have shown that mutated or dysfunctional FBW7 is associated with increase in c-Myc levels in breast cancer cells (29). Results in the present study show that γ-tocotrienol

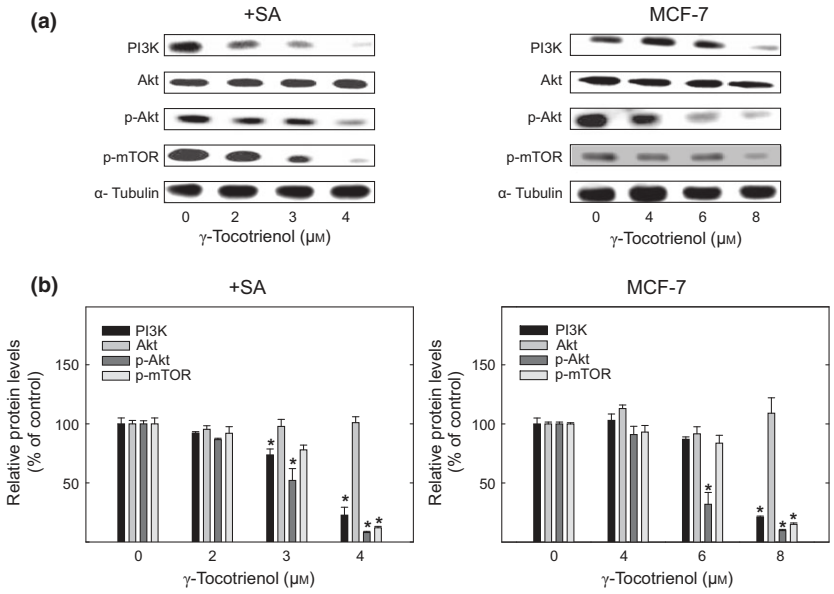

Figure 9. Western blot analysis of γ-tocotrienol effects on the PI3K/Akt/mTOR mitogenic signalling in +SA and MCF-7 mammary tumour cells. (a) +SA and MCF-7 cells were divided into different groups and treated with 0–4 μM (+SA) or 0–8 μM (MCF-7) γ-tocotrienol for 4-day treatment period. Afterwards, whole cell lysates were prepared for subsequent separation by polyacrylamide gel electrophoresis (50 μg/lane) followed by western blot analysis for PI3K (p110), Akt, phospho-Akt (p-Akt) and phospho-mTOR (p-mTOR). Visualization of α-tubulin was used to ensure equal sample loading in each lane. All experiments were repeated at least three times. (b) Scanning densitometric analysis was performed in triplicate on all blots and the integrated optical density of each band was normalized with corresponding α-tubulin levels, as shown in bar graphs below their respective western blot images. Vertical bars indicate the normalized integrated optical density of bands visualized in each lane ± SEM. $^*P < 0.05$ compared to their respective vehicle-treated control groups.

treatment induced reduction in phospho-GSK3α/β (inactive) and corresponding increase in p-T58-c-Myc and FWB7 levels. Furthermore, inhibition of GSK3α/β activity with LiCl was found to result in nearly complete blockade in γ-tocotrienol-induced reductions in c-Myc levels. Phosphatase PP2A and the peptidyl-prolyl cis/trans isomerase Pin 1 have also been shown to modulate c-Myc levels, and reduction in PP2A and/or Pin 1 has been shown to enhance tumour cell growth and malignant phenotype (28,30). However, γ-tocotrienol treatment was not found to affect PP2A or Pin 1 levels in +SA and MCF-7 mammary tumour cells, here. Taken together, these findings suggest that disinhibition of GSK3α/β plays a primary role in mediating inhibitory effects of γ-tocotrienol on c-Myc expression in +SA and MCF-7 mammary tumour cells. The terminal step in c-Myc metabolic degradation involves proteasomal degradation. Pre-treatment with proteasome inhibitor MG132 prior to γ-tocotrienol exposure resulted in nearly complete blockade of inhibitory effects of γ-tocotrienol on c-Myc levels, and indicates that intact proteasomal function was also required for γ-tocotrienol-induced c-Myc degradation.

Receptor tyrosine kinases also play an important role in regulation of c-Myc activity by activating mitogenic and survival signalling pathways including those of Ras/MEK/Erk and PI3K/Akt/mTOR (31). Stimulation of these is also associated with increase in c-Myc activity and stability, and reduction in c-Myc degradation (31). Elevations in oncogenic c-Myc levels has also been shown to be associated with spontaneous mutation of Ras family of proto-oncogenes, suggesting that aberrant c-Myc activity in mammary cells requires additional oncogene activation for expression of the malignant phenotype (3,32). Previous studies have shown that anti-cancer effects of γ-tocotrienol are associated with suppression of Ras/MEK/Erk and PI3K/Akt/mTOR mitogenic signalling (13,33). Results in the present study confirm and extend these findings, and indicate that γ-tocotrienol-dependent suppression in Ras/MEK/Erk and PI3K/Akt/mTOR mitogenic signalling displays a direct relationship with reduction in phosphorylated GSK3α/β (inactive form) and subsequent increase in GSK3α/β-mediated promotion of c-Myc ubiquitination and degradation.

Mitogen-dependent cell cycle progression is a highly organized and tightly regulated process, and includes G1, S, G2 and M phases (34). Passage through each phase is controlled by cyclin-dependent kinases (CDKs) and cell-dependent kinase inhibitors (CDKIs) (34). Early

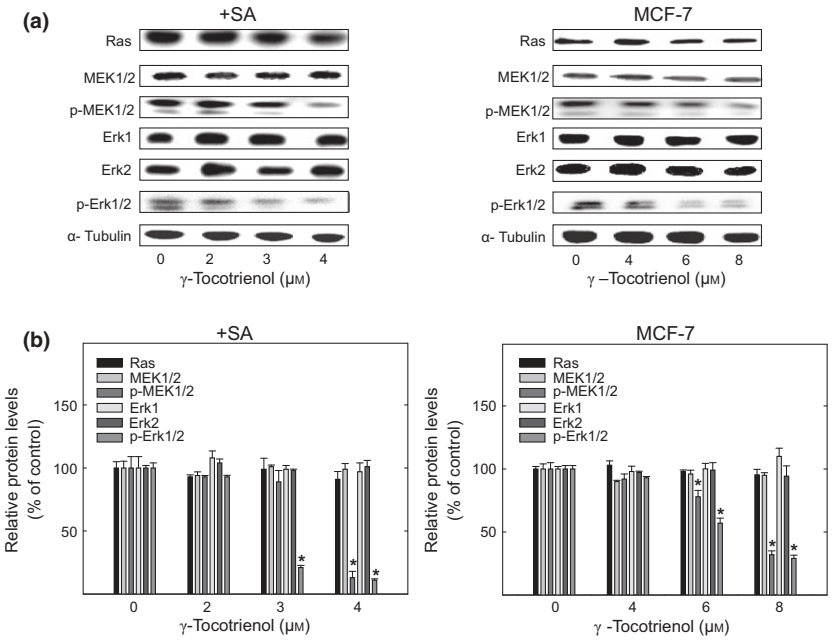

Figure 10. Western blot analysis of γ-tocotrienol effects on Ras/MEK/Erk mitogenic signalling in +SA and MCF-7 mammary tumour cells. (a) +SA and MCF-7 cells were divided into different groups and treated with 0–4 μM (+SA) or 0–8 μM (MCF-7) γ-tocotrienol for 4-day treatment period. Afterwards, whole cell lysates were prepared for subsequent separation by polyacrylamide gel electrophoresis (50 μg/lane) followed by western blot analysis for Ras, MEK1/2, phospho-MEK1/2 (p-MEK1/2), Erk1, Erk2 and phospho-Erk1/2 (p-Erk1/2). Visualization of α-tubulin was used to ensure equal sample loading in each lane. All experiments were repeated at least three times. (b) Scanning densitometric analysis was performed in triplicate on all blots and the integrated optical density of each band was normalized with corresponding α-tubulin levels, as shown in bar graphs below their respective western blot images. Vertical bars indicate the normalized integrated optical density of bands visualized in each lane ± SEM. $*P < 0.05$ compared to their respective vehicle-treated control groups.

in G1, there are increases in cyclin D and cyclin E expression. Cyclin D binds and activates CDK4/6 complex, while cyclin E binds and activates CDK2. These cyclin/CDK complexes then phosphorylate (inactivate) the cell cycle restriction protein, retinoblastoma (Rb), thereby releasing E2F transcription factors and leading to transcription of genes required for progression of the cell cycle from G1 to S (34,35). The CDKI, p27, binds to and inactivates cyclin/CDK complexes and inhibits cell cycle progression (34). c-Myc is one of the effectors that is directly involved in mitogen-dependent cell cycle progression (35). c-Myc stimulates transcription of CDK4, cyclin D1 and E2F1, and also acts to suppress activation of p27 (35,36). Results show that anti-proliferative effects of γ-tocotrienol treatment are associated with reduction in CDK4, cyclin D1, phosphorylated Rb, E2F1, and increasing p27 in +SA and MCF-7 mammary tumour cells.

It is well established that aberrant c-Myc signalling is a characteristic found in many forms of malignancy, particularly breast cancer (3,4,37). Thus, targeting c-Myc has attracted much attention as a therapeutic strategy for treatment of cancer. However, direct inhibition of c-Myc is difficult due to absence of a clear ligand-binding domain, and developing small-molecule inhibitors to disrupt formation of c-Myc and Max heterodimers is very challenging due to the heterodimer complex lacking a hydrophobic pocket (37,38). At present, there are no effective agents used clinically that directly inhibit c-Myc signalling (39). Alternative strategies for targeting c-Myc are currently under investigation (39). One possible alternative is the use of natural products, such as γ-tocotrienol, to enhance ubiquitination and degradation of c-Myc in cancer cells. In normal cells, c-Myc levels remain low by the highly organized serial phosphorylation of c-Myc that initially involves phosphorylation and activation of c-Myc at serine 62 (6,7). The resulting p-S62-c-Myc is a stable and active form of c-Myc that is further processed by Pin1, PP2A and GSK3β that ultimately leads to phosphorylation of c-Myc at threonine 58 and an unstable product that is now susceptible to polyubiquitination by E3 ubiquitin ligase Fbw7 and proteasomal degradation (6,7). The present findings demonstrates for the first time that exposure to γ-tocotrienol significantly reduced the ratio of p-S62-c-Myc to p-T58-c-Myc in breast cancer cells. This novel finding strongly suggests that γ-tocotrienol may provide an

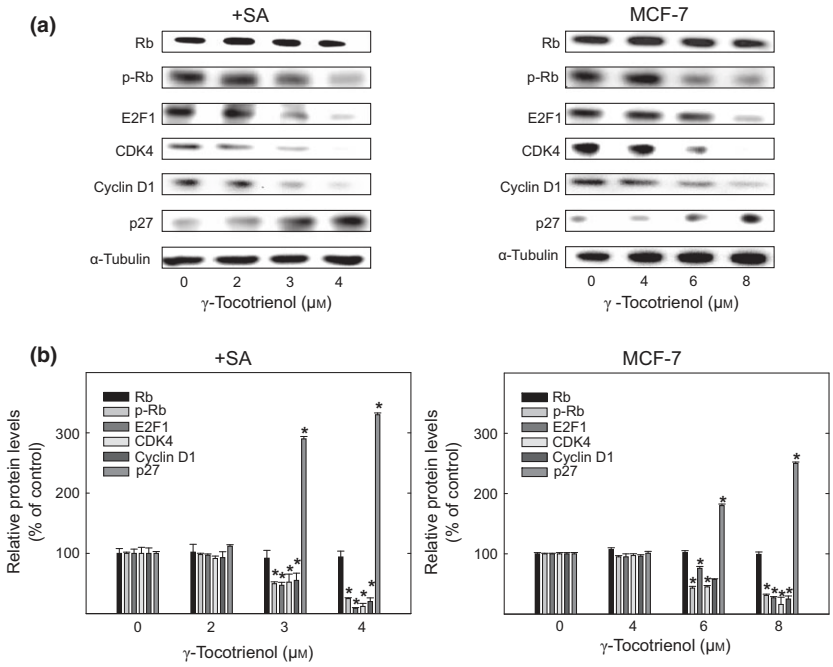

Figure 11. Western blot analysis of γ-tocotrienol effects cell cycle progression proteins in +SA and MCF-7 mammary tumour cells. (a) +SA and MCF-7 cells were divided into different groups and maintained on mitogen-free media containing 0–4 μM (+SA) or 0–8 μM (MCF-7) γ-tocotrienol for 48 h to establish cell cycle synchronization in all groups. All cells were then exposed to 100 ng/ml EGF for a 24-h period, whole cell lysates were prepared for subsequent separation by polyacrylamide gel electrophoresis (50 μg/lane) followed by western blot analysis for Rb, phospho-Rb (p-Rb), E2F1, CDK4, Cyclin D1 and p27. Visualization of α-tubulin was used to ensure equal sample loading in each lane. All experiments were repeated at least three times. (b) Scanning densitometric analysis was performed in triplicate on all blots and the integrated optical density of each band was normalized with corresponding α-tubulin levels, as shown in bar graphs below their respective western blot images. Vertical bars indicate the normalized integrated optical density of bands visualized in each lane ± SEM. *$P < 0.05$ compared to their respective vehicle-treated control groups

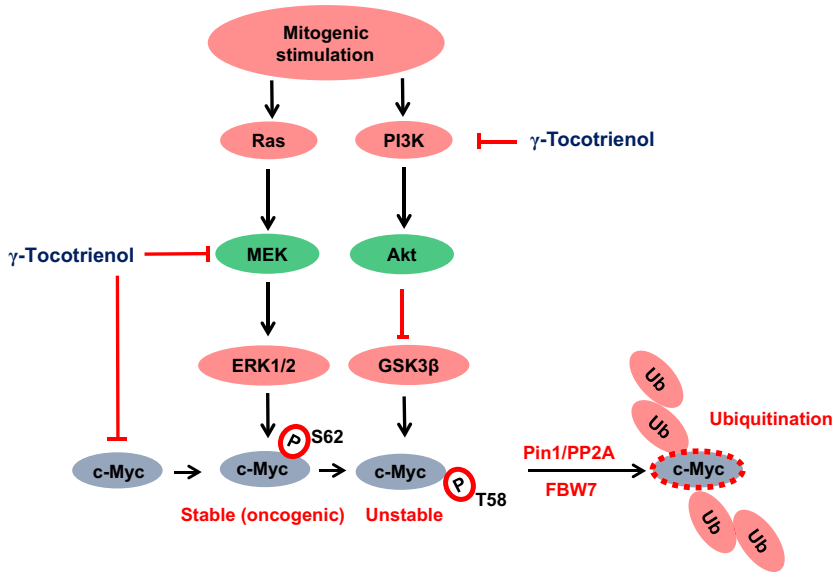

Figure 12. Schematic representation of γ-tocotrienol induced suppression and degradation of c-Myc protein in mammary tumour cells. γ-tocotrienol reduced stabilization of c-Myc by reducing p-Mek1/2 (activated) and p-Erk1/2 (activated) resulting in significantly large reduction in p-S62-c-Myc (stable). γ-tocotrienol also acted to reduce p-Akt (activated) leading to disinhibition of GSK3β, which resulted in increase in p-T58-c-Myc (unstable) and facilitated ubiquitination and degradation of c-Myc.

attractive alternative strategy to target aberrant c-Myc activation in the treatment of breast and possibly other types of cancer. A schematic representation of γ-tocotrienol-induced suppression and degradation of c-Myc protein in mammary tumour cells is summarized in Fig. 12.

Acknowledgements

This work was supported in part by grants from First Tec International Ltd. (Hong Kong), the Malaysian Palm Oil Council (MPOC), the Louisiana Cancer Foundation and the Louisiana Campuses Research Initiative (LACRI). The authors also thank Dr. Karen P. Briski, Fahad Alenazi and Pratistha Tamrakar for their generous technical assistance in using the iCycler iQ multicolor Real-Time PCR system and the laser confocal microscope.

References

1 Amati B, Brooks MW, Levy N, Littlewood TD, Evan GI, Land H (1993) Oncogenic activity of the c-Myc protein requires dimerization with Max. *Cell* **72**, 233–245.
2 Meyer N, Penn LZ (2008) Reflecting on 25 years with MYC. *Nat. Rev. Cancer* **8**, 976–990.
3 D'Cruz CM, Gunther EJ, Boxer RB, Hartman JL, Sintasath L, Moody SE *et al.* (2001) c-MYC induces mammary tumorigenesis by means of a preferred pathway involving spontaneous Kras2 mutations. *Nat. Med.* **7**, 235–239.
4 Hynes NE, Stoelzle T (2009) Key signalling nodes in mammary gland development and cancer: Myc. *Breast Cancer Res.* **11**, 210.
5 Wang YH, Liu S, Zhang G, Zhou CQ, Zhu HX, Zhou XB *et al.* (2005) Knockdown of c-Myc expression by RNAi inhibits MCF-7 breast tumor cells growth in vitro and in vivo. *Breast Cancer Res.* **7**, R220–R228.
6 Junttila MR, Westermarck J (2008) Mechanisms of MYC stabilization in human malignancies. *Cell Cycle* **7**, 592–596.
7 Sears RC (2004) The life cycle of C-myc: from synthesis to degradation. *Cell Cycle* **3**, 1133–1137.
8 Cantley LC (2002) The phosphoinositide 3-kinase pathway. *Science* **296**, 1655–1657.
9 Zhang X, Farrell AS, Daniel CJ, Arnold H, Scanlan C, Laraway BJ *et al.* (2012) Mechanistic insight into Myc stabilization in breast cancer involving aberrant Axin1 expression. *Proc. Natl Acad. Sci. USA* **109**, 2790–2795.
10 McIntyre BS, Briski KP, Gapor A, Sylvester PW (2000) Antiproliferative and apoptotic effects of tocopherols and tocotrienols on preneoplastic and neoplastic mouse mammary epithelial cells. *Proc. Soc. Exp. Biol. Med.* **224**, 292–301.
11 Tiwari RV, Parajuli P, Sylvester PW (2014) gamma-Tocotrienol-induced autophagy in malignant mammary cancer cells. *Exp. Biol. Med. (Maywood)* **239**, 33–44.
12 Ayoub NM, Akl MR, Sylvester PW (2013) Combined gamma-tocotrienol and Met inhibitor treatment suppresses mammary cancer cell proliferation, epithelial-to-mesenchymal transition and migration. *Cell Prolif.* **46**, 538–553.
13 Bachawal SV, Wali VB, Sylvester PW (2010) Combined gamma-tocotrienol and erlotinib/gefitinib treatment suppresses Stat and Akt signaling in murine mammary tumor cells. *Anticancer Res.* **30**, 429–437.
14 Sylvester PW, Ayoub NM (2013) Tocotrienols target PI3K/Akt signaling in anti-breast cancer therapy. *Anticancer Agents Med. Chem.* **13**, 1039–1047.
15 Sun W, Wang Q, Chen B, Liu J, Liu H, Xu W (2008) Gamma-tocotrienol-induced apoptosis in human gastric cancer SGC-7901 cells is associated with a suppression in mitogen-activated protein kinase signalling. *Br. J. Nutr.* **99**, 1247–1254.
16 Xu W, Du M, Zhao Y, Wang Q, Sun W, Chen B (2012) gamma-Tocotrienol inhibits cell viability through suppression of beta-catenin/Tcf signaling in human colon carcinoma HT-29 cells. *J. Nutr. Biochem.* **23**, 800–807.
17 Anderson LW, Danielson KG, Hosick HL (1981) Metastatic potential of hyperplastic alveolar nodule derived mouse mammary tumor cells following intravenous inoculation. *Eur. J. Cancer Clin. Oncol.* **17**, 1001–1008.
18 Danielson KG, Anderson LW, Hosick HL (1980) Selection and characterization in culture of mammary tumor cells with distinctive growth properties in vivo. *Cancer Res.* **40**, 1812–1819.
19 Malaviya A, Sylvester PW (2014) Synergistic Antiproliferative Effects of Combined gamma -Tocotrienol and PPAR gamma Antagonist Treatment Are Mediated through PPAR gamma -Independent Mechanisms in Breast Cancer Cells. *PPAR Res.* **2014**, 439146.
20 Akl MR, Ayoub NM, Abuasal BS, Kaddoumi A, Sylvester PW (2013) Sesamin synergistically potentiates the anticancer effects of gamma-tocotrienol in mammary cancer cell lines. *Fitoterapia* **84**, 347–359.
21 Samant GV, Wali VB, Sylvester PW (2010) Anti-proliferative effects of gamma-tocotrienol on mammary tumour cells are associated with suppression of cell cycle progression. *Cell Prolif.* **43**, 77–83.
22 Wali VB, Bachawal SV, Sylvester PW (2009) Suppression in mevalonate synthesis mediates antitumor effects of combined statin and gamma-tocotrienol treatment. *Lipids* **44**, 925–934.
23 Towbin H, Staehelin T, Gordon J (1979) Electrophoretic transfer of proteins from polyacrylamide gels to nitrocellulose sheets: procedure and some applications. *Proc. Natl Acad. Sci. USA* **76**, 4350–4354.
24 Urruticoechea A, Smith IE, Dowsett M (2005) Proliferation marker Ki-67 in early breast cancer. *J. Clin. Oncol.* **23**, 7212–7220.
25 Yap SP, Yuen KH, Wong JW (2001) Pharmacokinetics and bioavailability of alpha-, gamma- and delta-tocotrienols under different food status. *J. Pharm. Pharmacol.* **53**, 67–71.
26 Kang J, Sergio CM, Sutherland RL, Musgrove EA (2014) Targeting cyclin-dependent kinase 1 (CDK1) but not CDK4/6 or CDK2 is selectively lethal to MYC-dependent human breast cancer cells. *BMC Cancer* **14**, 32.
27 Gregory MA, Qi Y, Hann SR (2003) Phosphorylation by glycogen synthase kinase-3 controls c-myc proteolysis and subnuclear localization. *J. Biol. Chem.* **278**, 51606–51612.
28 Welcker M, Orian A, Jin J, Grim JE, Harper JW, Eisenman RN *et al.* (2004) The Fbw7 tumor suppressor regulates glycogen synthase kinase 3 phosphorylation-dependent c-Myc protein degradation. *Proc. Natl Acad. Sci. USA* **101**, 9085–9090.
29 Welcker M, Clurman BE (2008) FBW7 ubiquitin ligase: a tumour suppressor at the crossroads of cell division, growth and differentiation. *Nat. Rev. Cancer* **8**, 83–93.
30 Yeh E, Cunningham M, Arnold H, Chasse D, Monteith T, Ivaldi G *et al.* (2004) A signalling pathway controlling c-Myc degradation that impacts oncogenic transformation of human cells. *Nat. Cell Biol.* **6**, 308–318.
31 Xu J, Chen Y, Olopade OI (2010) MYC and Breast Cancer. *Genes Cancer* **1**, 629–640.
32 Sears R, Nuckolls F, Haura E, Taya Y, Tamai K, Nevins JR (2000) Multiple Ras-dependent phosphorylation pathways regulate Myc protein stability. *Genes Dev.* **14**, 2501–2514.
33 Shin-Kang S, Ramsauer VP, Lightner J, Chakraborty K, Stone W, Campbell S *et al.* (2011) Tocotrienols inhibit AKT and ERK activation and suppress pancreatic cancer cell proliferation by

suppressing the ErbB2 pathway. *Free Radic. Biol. Med.* **51**, 1164–1174.
34 Massague J (2004) G1 cell-cycle control and cancer. *Nature* **432**, 298–306.
35 Matsumura I, Tanaka H, Kanakura Y (2003) E2F1 and c-Myc in cell growth and death. *Cell Cycle* **2**, 333–338.
36 Pelengaris S, Khan M, Evan G (2002) c-MYC: more than just a matter of life and death. *Nat. Rev. Cancer* **2**, 764–776.
37 Nair SK, Burley SK (2003) X-ray structures of Myc-Max and Mad-Max recognizing DNA. Molecular bases of regulation by proto-oncogenic transcription factors. *Cell* **112**, 193–205.
38 Darnell JE Jr (2002) Transcription factors as targets for cancer therapy. *Nat. Rev. Cancer* **2**, 740–749.
39 Delmore JE, Issa GC, Lemieux ME, Rahl PB, Shi J, Jacobs HM *et al.* (2011) BET bromodomain inhibition as a therapeutic strategy to target c-Myc. *Cell* **146**, 904–917.